Electronic Supplementary Information

Metalloporphyrinic Metal-Organic Frameworks for Enhanced Photocatalytic Degradation of a Mustard Gas Simulant

Alisa S. Quon,[‡a] Doroteo Manriquez,[‡a] Anna Nguyen,[§a] Edgar K. Papazyan,[§a] Pavithra Wijeratne,[a] Lun An,[b] Long Qi,[b] Matthew J. Tang,[a] Austin D. Ready,[c] Omar K. Farha*[d] and Yangyang Liu*[a]

[a] Department of Chemistry and Biochemistry, California State University, Los Angeles, 5151 State University Drive, Los Angeles, California 90032, United States

[b] U.S. DOE Ames National Laboratory, Iowa State University, Ames, Iowa 50011, United States

[c] Department of Chemistry and Biochemistry, University of California, Los Angeles, 607 Charles E. Young Drive East, Los Angeles, California 90095, United States

[d] Department of Chemistry and International Institute for Nanotechnology (IIN) and Department of Chemical & Biological Engineering, Northwestern University, Evanston, Illinois 60208, United States

§ Current address: California University of Science and Medicine, Colton, California 92324, United States.

‡ A.S.Q. and D.M. contributed equally.

* *Email:* yliu114@calstatela.edu; o-farha@northwestern.edu

Table of Contents

Section S1. Materials and Instrumentation

Benzoic acid (99.5%), propionic acid (95%), methanol (MeOH, 99.8%), methanol-d_4 (CD_3OD, 99.8%), pyrrole (99%), chloroform ($CHCl_3$, 99.8%), dichloromethane (DCM, 99.5%), *N,N*-dimethylformamide (DMF, 99.9%), hydrochloric acid (HCl), pyridine (99%), anhydrous tetrahydrofuran (THF, 99.9%), glacial acetic acid, potassium hydroxide pellets (KOH, 85%), anhydrous magnesium sulfate ($MgSO_4$), methyl 4-formylbenzoate (98%), anhydrous indium(III) chloride ($InCl_3$, 99.99%), 4-carboxybenzaldehyde (98%), tin(II) chloride dihydrate ($SnCl_2 \cdot 2H_2O$, 98%), 2-aminobenzene-1,4-dicarboxylic acid (99%), sodium hydroxide (NaOH, 98%) and ammonium molybdate(VI) tetrahydrate (99%+) were purchased from Fisher Scientific. 1-bromo-3,5-difluorobenzene (98%), anhydrous zirconium(IV) chloride ($ZrCl_4$, 99.5%), and N,N-dimethyl-4-nitrosoaniline (DMNA, 98%) were purchased from Alfa Aesar. 9,10-Dimethylanthracene (DMA, 99%), potassium iodide (KI, 99%), and zirconium acetate solution in dilute acetic acid (15-17 wt% Zr) was purchased from Sigma Aldrich. *Meso*-tetra(4-carboxyphenyl)porphine (H_2TCPP, 97%) was purchased from Frontier Scientific. Benzene-1,4-dicarboxylic acid (>99%) was purchased from Acros Organics. 2-chloroethyl ethyl sulfide (CEES, >97%) and potassium hydrogen phthalate (99.8%) were purchased from TCI America. All reagents were used as received without further purification.

The nitrogen isotherms at 77 K and the Brunauer-Emmett-Teller (BET) surface areas of all MOF samples were measured on a Micromeritics ASAP 2020 Plus. Powder X-ray diffraction (PXRD) patterns were collected on a D2 Phaser (Bruker Corporation) equipped with a Cu sealed tube (λ = 1.54178) at 30 kV and 10 mA, a step size of 2θ = 0.02° (5 s per step) over a 2θ range of 2 to 20°. Scanning electron microscopy (SEM) images were acquired on an FEI Quanta-FEG 250 field-emission SEM microscope. The samples were pre-coated with 3 nm thick iridium before analysis. Thermogravimetric analysis (TGA) was conducted using a TA Instruments Discovery TGA 55. For each thermal curve, 3-5 mg of sample were placed on a 100 µL platinum pan and allowed to reach 700 °C at a ramp rate of 10 °C/min under nitrogen with a flow rate of 40 ml/min. The UV-vis spectra were recorded on a Shimadzu UV-2600 spectrophotometer equipped with ISR-2600 Integrating Sphere using 1 cm light path quartz cuvettes. The scan step was set as 1 nm. ^1H NMR spectroscopy was collected on a 400 MHz NMR spectrometer (Bruker Instruments). Gas chromatography-mass spectrometry (GC-MS) analysis was performed on an Agilent 8890-GC coupled with a 7000D MS/MS EI detector. LED irradiation was generated using solderless LEDs purchased from RapidLED, which were then mounted on aluminum to give a homemade irradiation setup. The LEDs were hooked up in series to a Mean Well LPC-35-700 constant current driver purchased from RapidLED. Each irradiation setup contains four CREE XT-E Royal Blue LEDs mounted facing each other ~3 cm apart (the power density of each blue LED is 200 mW/cm^2). Inductively coupled plasma-optical emission spectroscopy (ICP-OES) was collected on an Agilent 5110 ICP-OES with SPS 4 Autosampler. Five standard solutions (2, 5, 10, 20, and 50 ppm) were prepared through serial dilution to generate the calibration curve for each metal.

Section S2. Syntheses of Ligands and MOFs

Synthesis of M-TCPP (M = Sn, In). The metalloporphyrin Sn-TCPP was synthesized in two steps according to previous literature to yield a dark purple solid (Scheme S1).[1] In-TCPP was synthesized in three steps to yield a dark green solid (Scheme S2).[2]

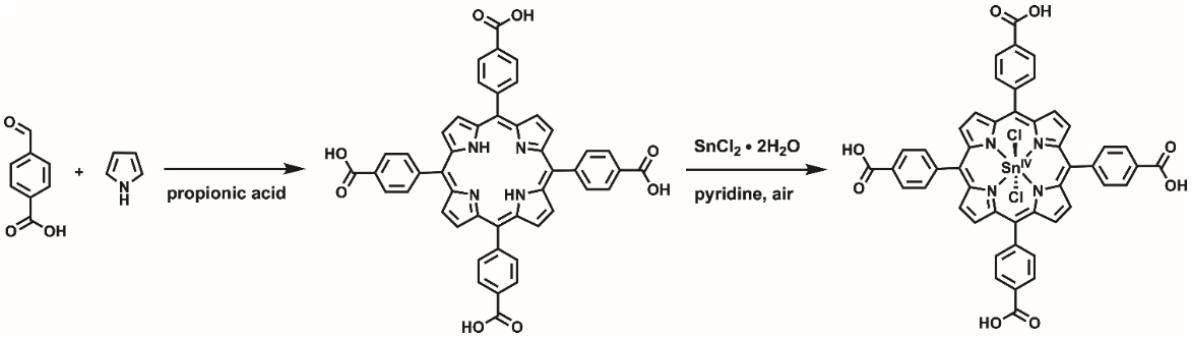

Scheme S1. Synthesis of Sn-TCPP.

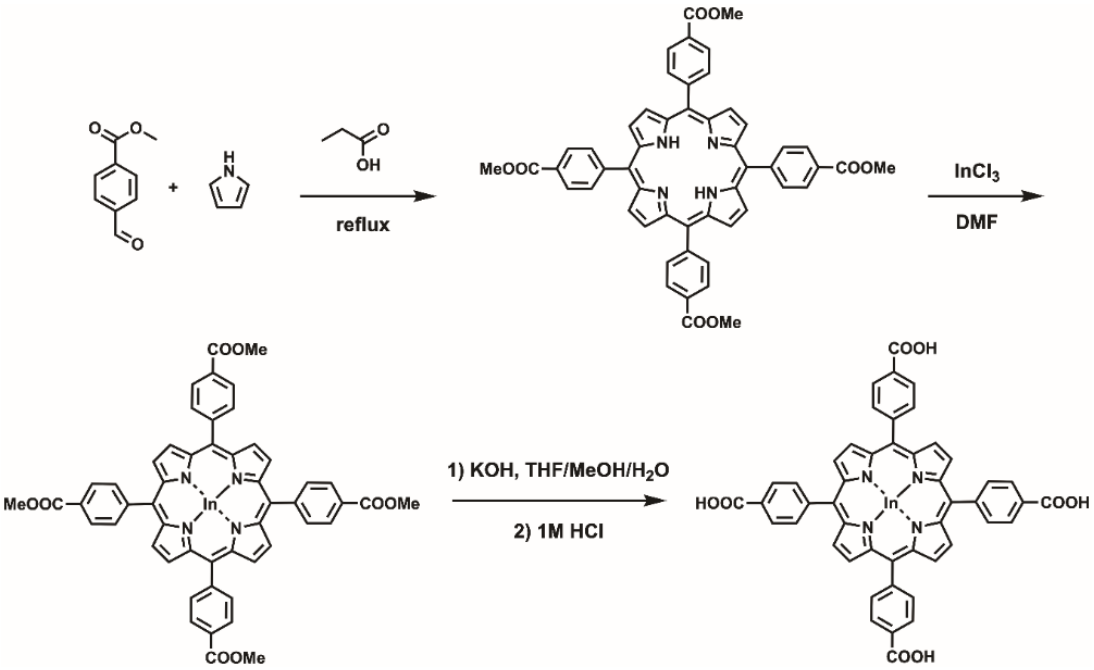

Scheme S2. Synthesis of In-TCPP.

Synthesis of PCN-222(M), M = Sn, In. The metalated PCN-222 MOFs were synthesized according to previously reported literature.[2] Anhydrous $ZrCl_4$ (70 mg), M-TCPPCl (50 mg), and benzoic acid (2700 mg) were dissolved in 8 mL of DMF in a 20 mL vial. The vials were sonicated for 30 minutes and incubated in an oven at 120 °C for 48 h. After cooling to room temperature, the suspensions were transferred to centrifuge tubes and washed with DMF (3 x 20 mL) and acetone (3 x 20 mL). After soaking in acetone overnight, the samples were dried in a vacuum oven (~80 kPa) overnight and then evacuated at 120 °C for 12 h on the activation port of a Micromeritics ASAP 2020 Plus.

Synthesis of CAU-26. CAU-26 was synthesized following a modified procedure reported by Leubner et al.[3] Benzene-1,4-dicarboxylic acid (232.6 mg, 1.40 mmol) and 20 mL of acetic acid were added to a Teflon-lined autoclave and sonicated until fully dissolved. Zirconium acetate solution (0.892 mL, 2 mmol) in dilute acetic acid (15-17 wt% Zr) was added, and the vessel was sonicated again. The mixture was then incubated in an oven at 160 °C for 22 h. The product was washed with DMF (3 x 20 mL) and acetone (3 x 20 mL) and dried in a vacuum oven (~80 kPa) overnight.

Synthesis of CAU-26-NH_2. CAU-26-NH_2 was synthesized following a modified procedure reported by Leubner et al.[3] 2-Aminobenzene-1,4-dicarboxylic acid (253.6 mg, 1.40 mmol) and 20 mL of acetic acid were added to a Teflon-lined autoclave and sonicated until fully dissolved. Zirconium acetate solution (0.892 mL, 2 mmol) in dilute acetic acid (15-17 wt% Zr) was added, and the vessel was sonicated again. The mixture was then incubated in an oven at 160 °C for 22 h. The product was washed with DMF (3 x 20 mL) and acetone (3 x 20 mL) and dried in a vacuum oven (~80 kPa) overnight.

Synthesis of CSLA-21(Sn). CSLA-21(Sn) was synthesized by dissolving Sn-TCPP (60 mg) in DMF (7 mL) via sonication for 20 minutes in a 20 mL scintillation vial. After sonication, CAU-26 (19 mg) was added, and the vial was incubated in an oven for 18 h at 65 °C. After cooling, the suspension was transferred to centrifuge tubes and washed with DMF (5 x 20 mL). The sample was allowed to sit overnight in DMF after the fifth wash. The following day, the washing was repeated with acetone (3 x 20 mL). After soaking in acetone overnight, the solvent was decanted, and the resulting powder was dried in a vacuum oven (~80 kPa) overnight and then evacuated at 60 °C for 6 h on the activation port of a Micromeritics ASAP 2020 Plus.

Synthesis of CSLA-21-NH_2(Sn). CSLA-21-NH_2(Sn) was synthesized by dissolving Sn-TCPP (55 mg) in DMF (7 mL) via sonication for 20 minutes in a 20 mL scintillation vial. After sonication, CAU-26-NH_2 (19 mg) was added, and the vial was incubated in an oven for 18 h at 65 °C. After cooling, the suspension was transferred to centrifuge tubes and washed with DMF (5 x 20 mL). The sample was allowed to sit overnight in DMF after the fifth wash. The following day, the washing was repeated with acetone (3 x 20 mL). After soaking in acetone overnight, the solvent was decanted, and the resulting powder was dried in a vacuum oven (~80 kPa) overnight and then evacuated at 60 °C for 6 h on the activation port of a Micromeritics ASAP 2020 Plus.

Section S3. Thermogravimetric Analysis (TGA)

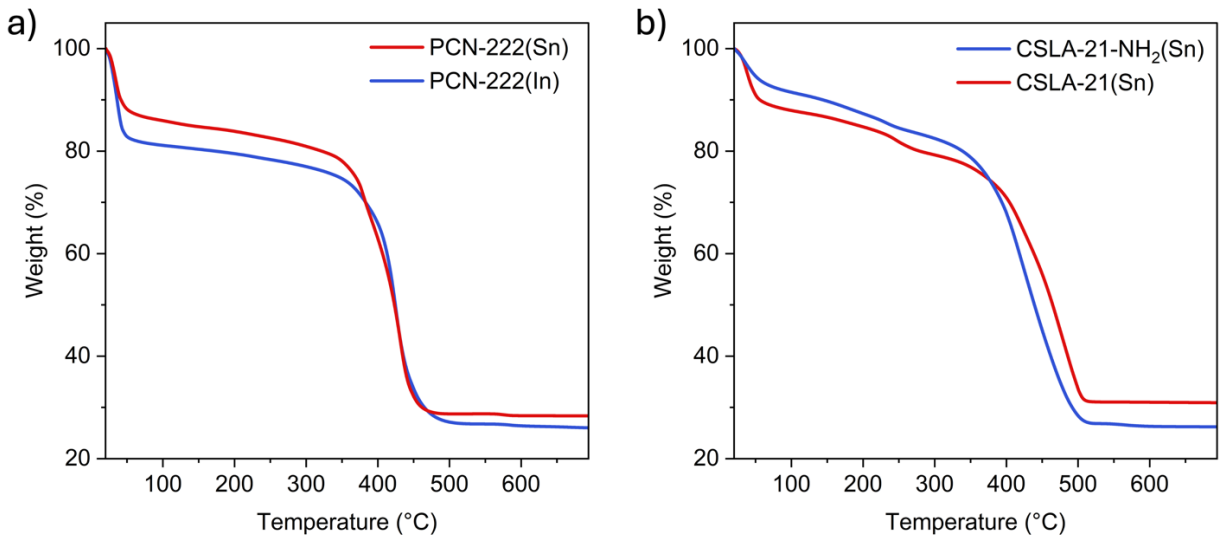

Figure S1. (a) TGA plots of PCN-222(Sn) and PCN-222(In). (b) TGA plots of CSLA-21(Sn) and CSLA-21-NH_2(Sn).

Section S4. Ultraviolet-Visible Spectroscopy

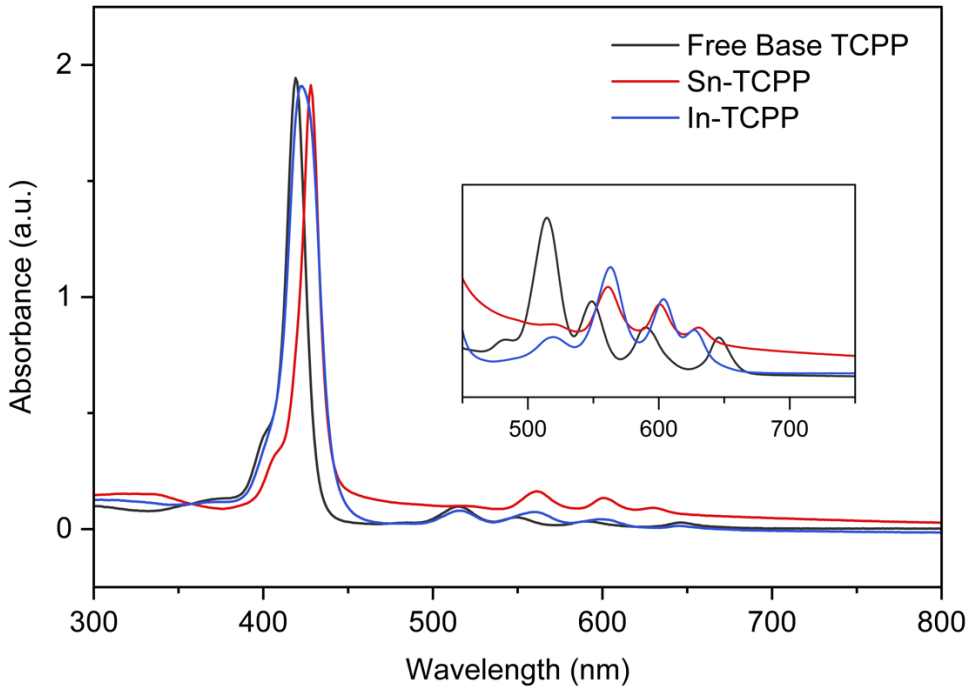

Figure S2. UV-vis spectra of free base tetrakis(4-carboxyphenyl)porphyrin (TCPP), Sn-TCPP, and In-TCPP. The spectra were collected without integrating sphere for the homogeneous solutions of TCPP, Sn-TCPP and In-TCPP.

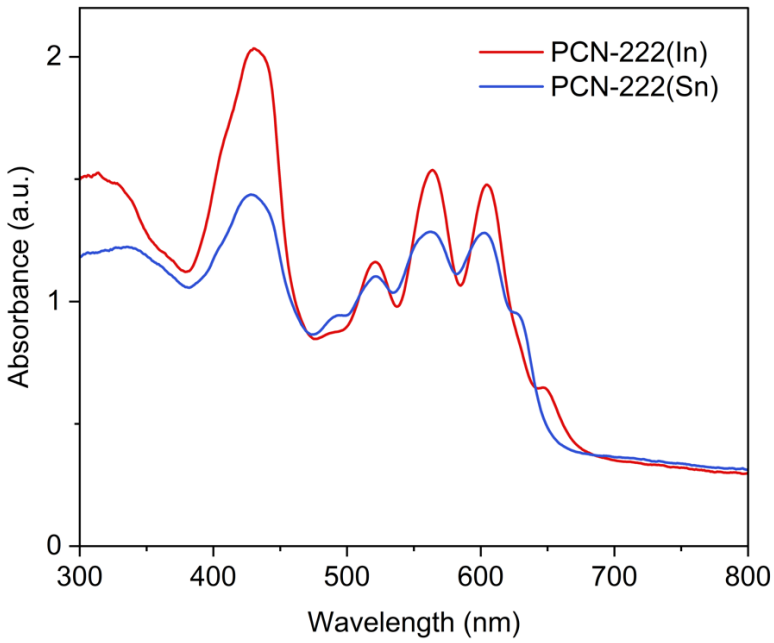

Figure S3. UV-vis spectra of PCN-222(Sn) and PCN-222(In) suspensions in MeOH. The spectra were collected using an integrating sphere for 0.002 mmol PCN-222(Sn) in 2 mL MeOH and 0.002 mmol PCN-222(In) in 3 mL MeOH.

Section S5. SEM images

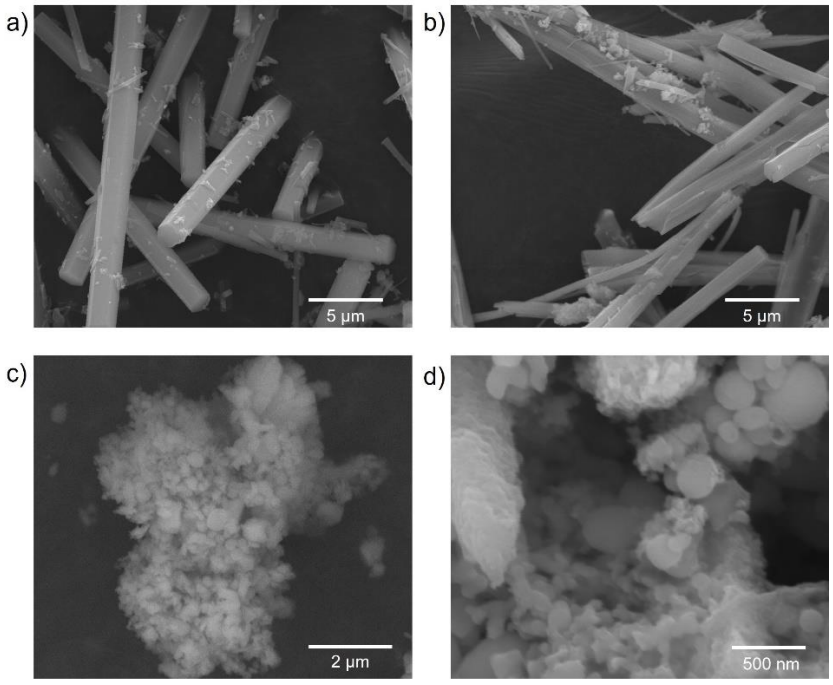

Figure S4. The SEM images of (a) PCN-222(Sn), (b) PCN-222(In), (c) CSLA-21(Sn), and (d) CSLA-21-NH_2(Sn).

Section S6. Kinetic Studies

Photooxidation Experiments. Photooxidation experiments were carried out using a method previously reported by our group.[4] To a microwave vial, 1 mL of methanol and 0.5 mol % (0.001 mmol) of catalyst were added. O_2 gas was bubbled into the vial for 20 min followed by blue LED irradiation for 20 minutes. An internal standard, 1-dibromo-3,5-difluorobenzene (5 µL, 0.04 mmol), and CEES (23 µL, 0.2 mmol) were added at t = 0 min. A sample from the vial was taken and diluted with 0.5 mL of dichloromethane (DCM) in a gas chromatography (GC) vial. The vial was irradiated with blue light again. GC samples were taken every few minutes depending on the catalyst, and all samples were analyzed with gas chromatography-mass spectrometry (GC-MS). The spectra were analyzed to calculate the percent conversion of CEES at each time point. These experiments were repeated in triplicate or until consistent data were obtained, and the average percent conversion of CEES at each time point was plotted against time for each catalyst.

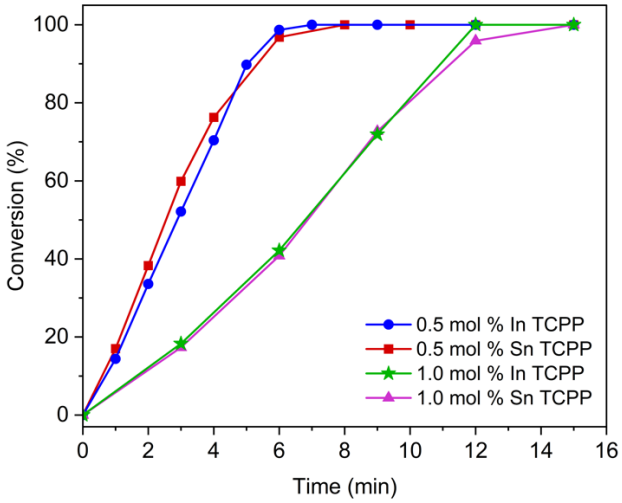

Figure S5. Percent conversion of CEES over time using 0.5 and 1.0 mol% of Sn-TCPP or In-TCPP as catalysts in methanol (homogeneous). At least three runs were carried out for each ligand, and the kinetic plots are the average of the three runs.

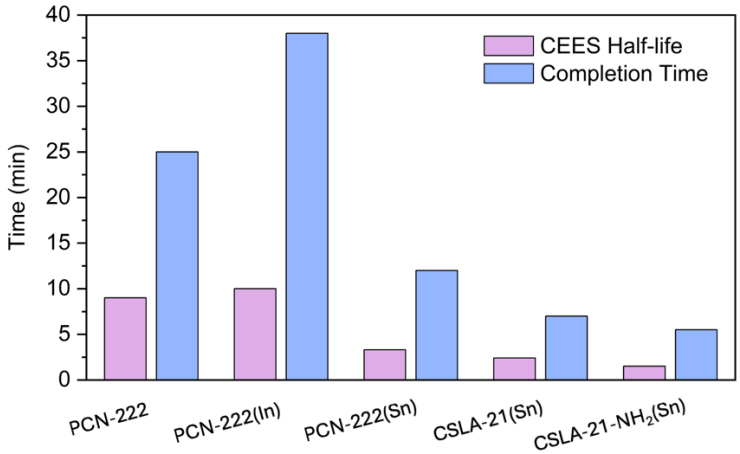

Figure S6. Comparison of CEES half-lives and oxidation completion times using 1.0 mol% PCN-222(H_2) and 0.5 mol% PCN-222(In), PCN-222(Sn), CSLA-21(Sn), and CSLA-21-NH_2(Sn).

Table S1. Comparison of CEES photooxidation rates and reaction conditions for top-performing MOFs.

MOF	Photosensitizer	Catalyst Loading (mol %)	$t_{1/2}$ (min)	Completion Time (min)	TOF (h^{-1})	O_2/Air	Solvent	LED source	Ref.
Au/TCPP@MIL-101(Cr)	Au NP / TCPP	1.8	0.75	1.5	N/A[b]	O_2	MeOH	Blue	[5]
TCPP@MIL-101(Cr)	TCPP	1.8	1	2	N/A	O_2	MeOH	Blue	[5]
ZZU-602	Zn-TCPP	1	1.1	5	N/A	O_2	MeOD	White	[6]
TCPP@Zr-BTB MOL	TCPP, BTB	0.16	1.2	4	N/A	O_2	MeCN	Violet	[7]
ZnTPP@ZIF-8	ZnTPP	0.5	1.5	4	N/A	Air	MeOH	Blue	[8]
Ag_{12}TPyP	TPyP	1	1.5	5	N/A	O_2	MeOD	White	[9]
CSLA-21-NH_2(Sn)	**Sn-TCPP**	**0.5**	**1.5**	**5.5**	**2,182**	**O_2**	**MeOH**	**Blue**	**This Work**
BUT-233	H_4BBCPPP-Ph	0.75	2	5	N/A	O_2	MeOD	White	[10]
PPIX@NU-1000	Protoporphyrin IX, pyrene	0.7	2.1	10	N/A	O_2	MeCN	Blue	[11]
BrBDP@NU-1000	BODIPY, pyrene	0.2	2.3	6	N/A	O_2	MeOH	Green	[12]
PPIX@Zr-BTB MOL	Protoporphyrin IX, BTB	0.39	2.3	6	N/A	O_2	MeCN	Violet	[7]
ZZU-601	TCPP	1	2.3	6	N/A	O_2	MeOD	White	[6]
CSLA-21(Sn)	**Sn-TCPP**	**0.5**	**2.4**	**7**	**1,714**	**O_2**	**MeOH**	**Blue**	**This Work**
Fe-TCPP-La	Fe(II)-TCPP	1	2.5	5	N/A	O_2	MeOH	Blue	[13]
UiO-68-TBTD	Triazolobenzothia-diazole	0.2	3	10	N/A	Air	MeOH	Blue	[14]
PCN-222(Sn)	**Sn-TCPP**	**0.5**	**3.3**	**12**	**1,000**	**O_2**	**MeOH**	**Blue**	**This Work**
NU-1000-PCBA	Pyrene, C_{60}	0.7	3.5	14	N/A	O_2	MeOH	UV	[15]
Ni-TCPP-La	Ni-TCPP	1	3.5	7	N/A	O_2	MeOH	Blue	[13]
PCN-57-Se	Benzoselenadiazole	0.1	3.5	12	N/A	O_2	MeOH	Violet	[16]
UMCM-313	Perylene	0.5	4	12	840	O_2	MeOH	Blue	[17]
TCPP-La	TCPP	1	4	7	N/A	O_2	MeOH	Blue	[13]
Zn-TCPP-La	Zn-TCPP	1	4	8	N/A	O_2	MeOH	Blue	[13]
PP@Al-PMOF textile	TCPP	0.2	4	45	10,200	O_2	MeOH	Blue	[18]
I_2-BODIPY@ZIF-8	I_2-BODIPY	1.25	4.5	12	N/A	O_2	MeOH	Green	[19]
Mn-TCPP-La	Mn-TCPP	1	5	10	N/A	O_2	MeOH	Blue	[13]
Co-TCPP-La	Co-TCPP	1	5.5	11	N/A	O_2	MeOH	Blue	[13]
NU-1000-*o*-$(Cl)_4$	Pyrene	1	5.5	8	N/A	O_2	MeOH	UV	[20]
NU-1000	Pyrene	1	6	15	N/A	O_2	MeOH	UV	[21]
MOF-525	TCPP	1	6.2	15	800	O_2	MeOH	Blue	[4]
PCN-57-S	Benzothiadiazole	0.1	7.5	25	N/A	O_2	MeOH	UV	[16]
PCN-222(H_2)	TCPP	1	9[a]	25	480	O_2	MeOH	Blue	[4]
BUT-223	H_4BBCPPP	0.75	9	20	N/A	O_2	MeOD	White	[10]
PCN-222(In)	**In-TCPP**	**0.5**	**10**	**38**	**317**	**O_2**	**MeOH**	**Blue**	**This Work**
Al-PMOF	TCPP	0.7	16	120	540	O_2	MeOH	Blue	[18]

[a] Fastest reported CEES half-life for PCN-222(H_2)
[b] Turnover frequency (TOF) not reported

Section S7. Sulfoxide Selectivity Studies and ^{1}H NMR Analysis

To a microwave vial, 1 mL of CD_3OD and 0.5 mol % (0.001 mmol) of catalyst were added. O_2 gas was bubbled into the microwave vial for 20 min followed by irradiation with blue LED light for 20 min. CEES (23 µL, 0.2 mmol) was added at t = 0 min. The microwave vial was irradiated with blue light again until 100% CEES conversion was reached, which was confirmed by GC-MS analysis on a sample taken from the vial. The solution was filtered to remove MOF and then analyzed using ^{1}H NMR to determine the sulfoxide selectivity:

$$sulfoxide\ selectivity = \frac{integration_{sulfoxides}}{integration_{sulfoxides} + integration_{sulfone}} \times 100\%$$

A sample annotated ^{1}H NMR for PCN-222(Sn) sulfoxide selectivity in methanol-d_4 is shown in Figure S7. A small amount of ethyl vinyl sulfoxide (EVSO), another nontoxic product, was generated alongside CEESO.

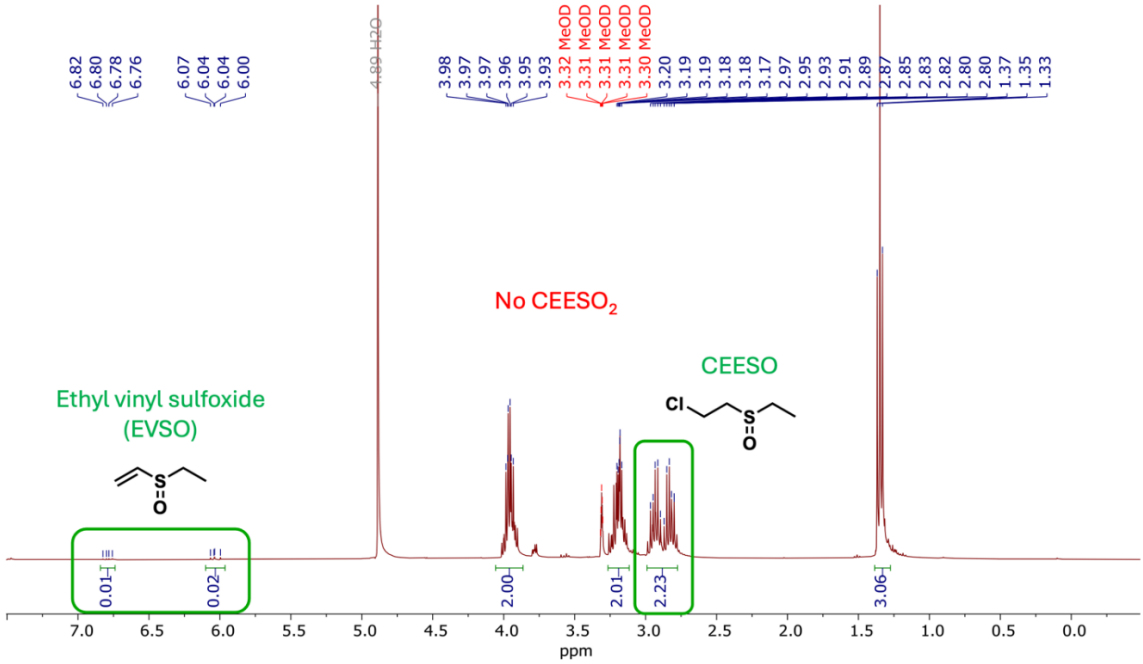

Figure S7. ^{1}H NMR spectrum in CD_3OD after 100% CEES conversion with PCN-222(Sn).

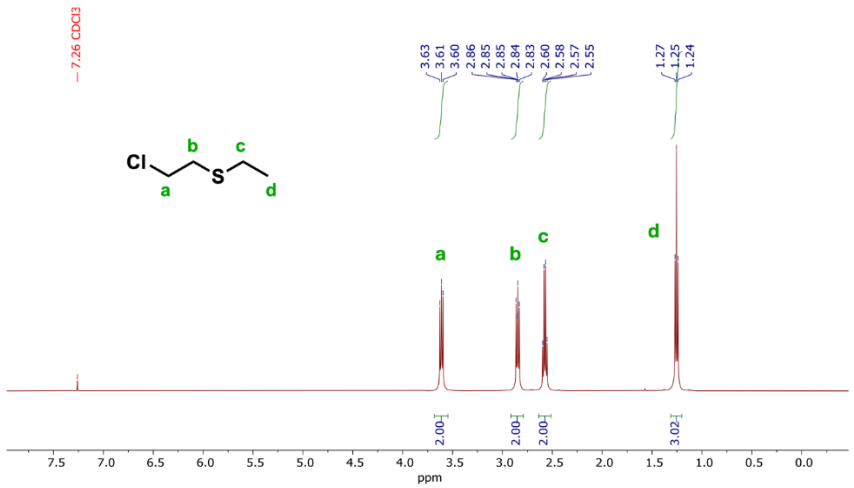

Figure S8. ^{1}H NMR spectrum of pure CEES in $CDCl_3$.

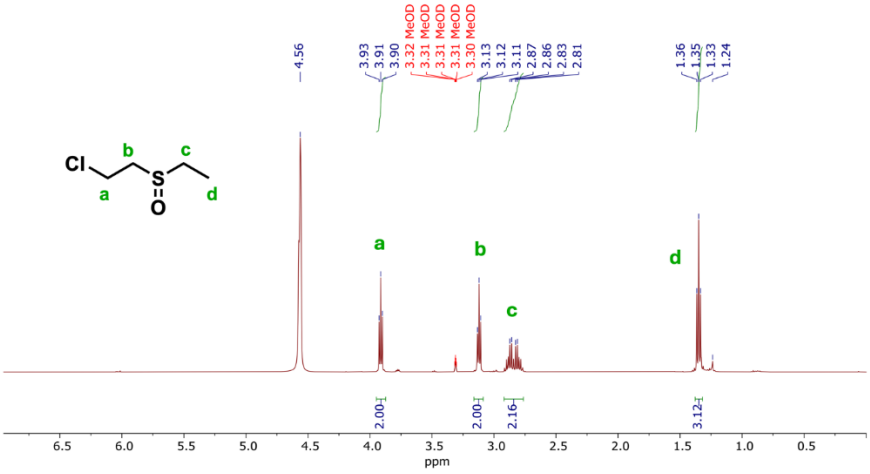

Figure S9. ^{1}H NMR spectrum of pure CEESO in $CDCl_3$.

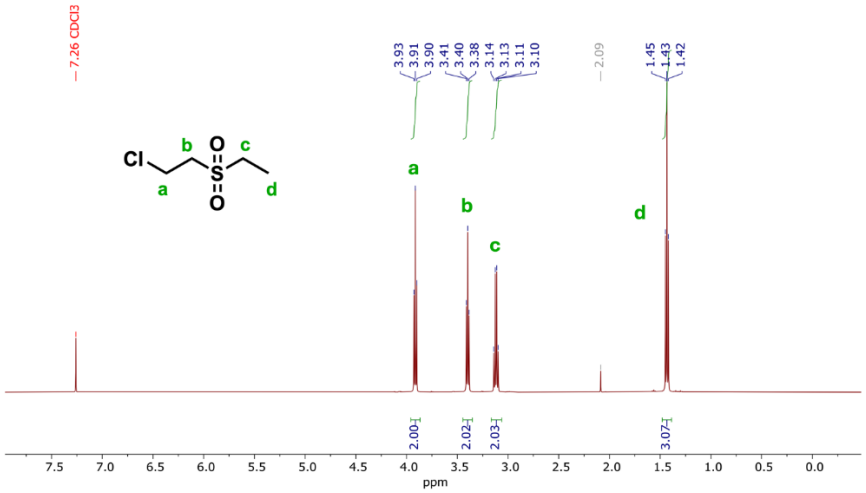

Figure S10. ^{1}H NMR spectrum of pure $CEESO_2$ in $CDCl_3$.

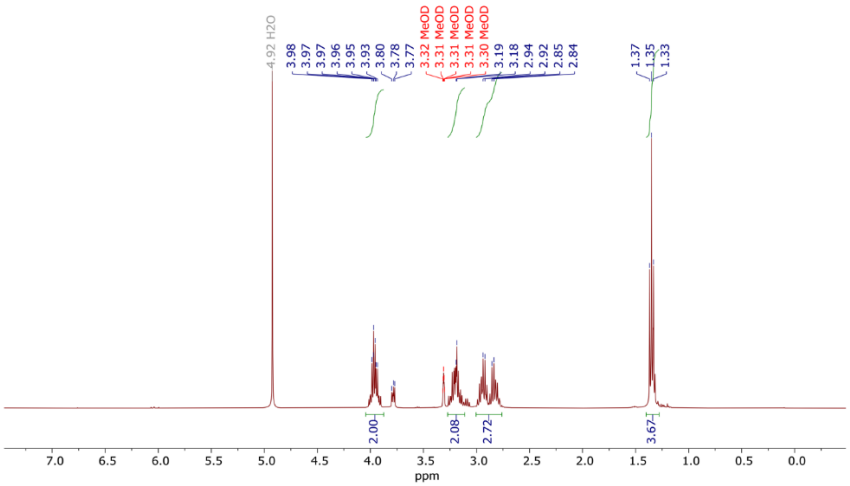

Figure S11. ^{1}H NMR spectrum of CEES oxidation reaction in CD_3OD in the presence of 0.5 mol% PCN-222(In) under blue LED after 100% CEES conversion.

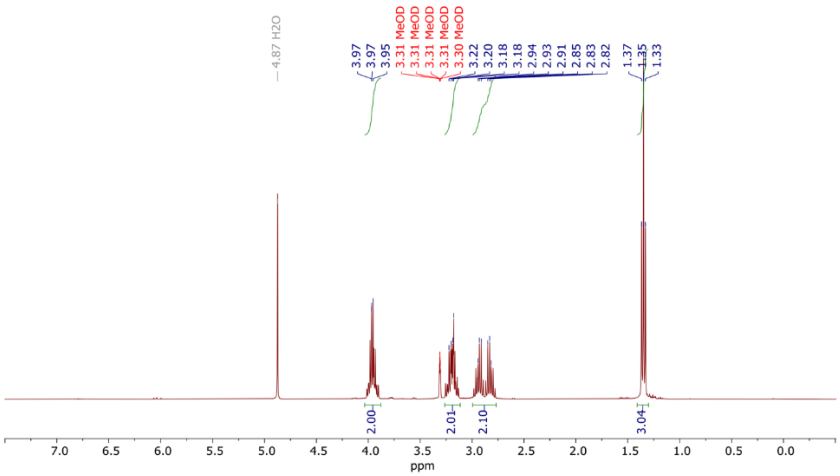

Figure S12. ^{1}H NMR spectrum of CEES oxidation reaction in CD_3OD in the presence of 0.5 mol% CSLA-21(Sn) under blue LED after 100% CEES conversion.

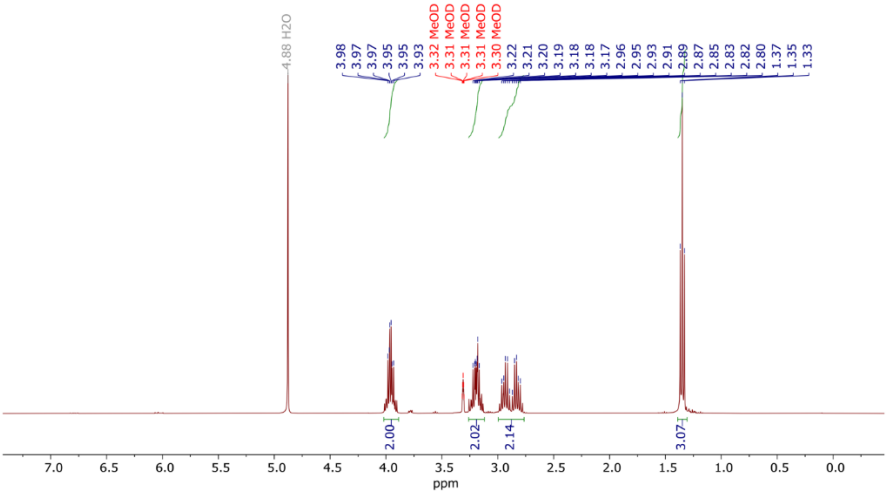

Figure S13. ^{1}H NMR spectrum of CEES oxidation reaction in CD_3OD in the presence of 0.5 mol% CSLA-21-NH_2(Sn) under blue LED after 100% CEES conversion.

Section S8. Post-catalysis PXRD

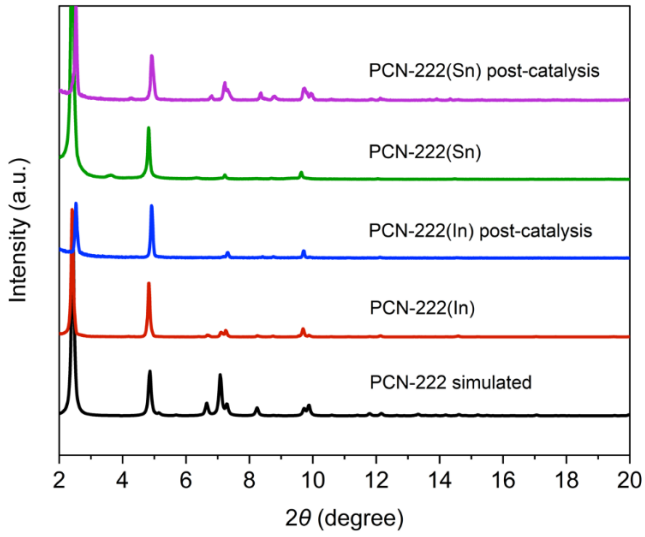

Figure S14. PXRD spectra of PCN-222(Sn) and PCN-222(In) before and after catalysis.

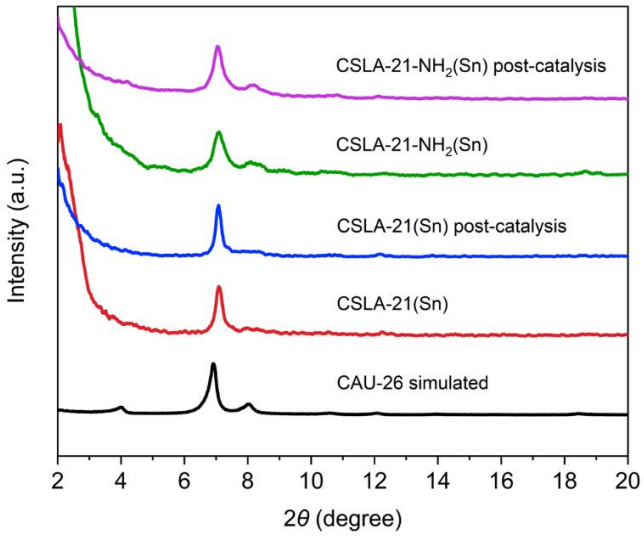

Figure S15. PXRD spectra of CSLA-21(Sn) and CSLA-21-NH_2(Sn) before and after catalysis.

Section S9. Recyclability Testing

The recyclability of each MOF was tested for up to 4 cycles. After the first completed reaction, the reaction vial was flushed with oxygen for 20 minutes, followed by the addition of 23 µL (0.2 mmol) of CEES. A sample of t = 0 was taken from the vial and prepared for GC analysis. The vial was then placed under blue light for the longest amount of time it took the respective MOF to achieve 100% conversion. A GC sample was prepared at the end of this period to determine if 100% conversion was achieved. If not, the sample was irradiated until completion. Once 100% conversion was achieved, the oxygenation, CEES addition, and blue light irradiation steps were repeated.

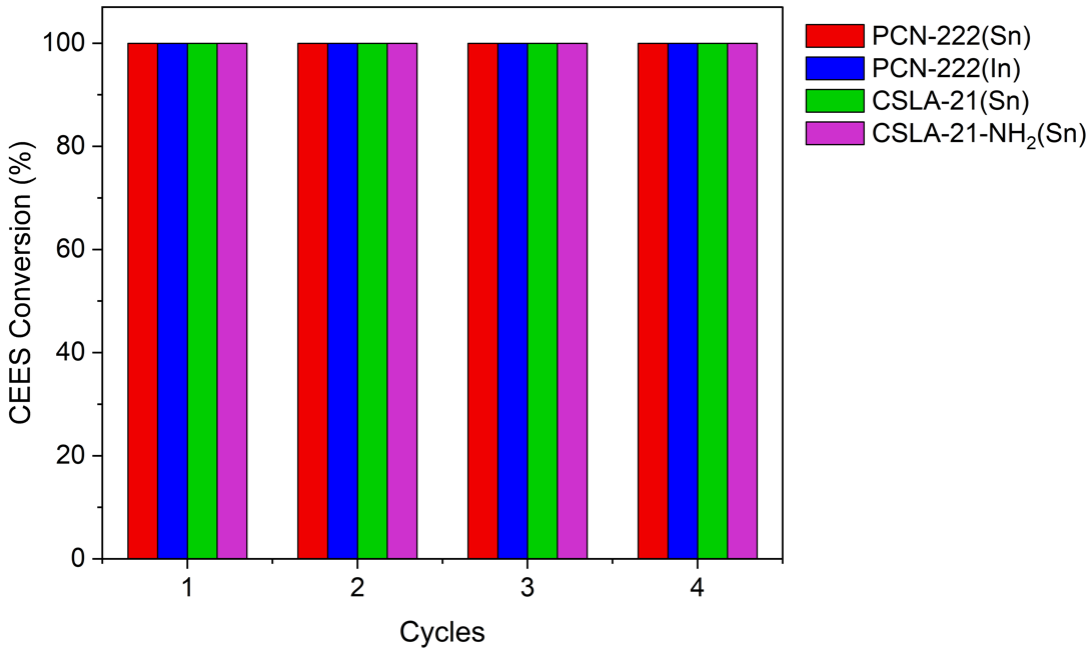

Figure S16. Recyclability of MOFs for CEES photooxidation up to 4 cycles.

ICP Analysis After Recyclability. Upon completion of four cycles of recyclability, the MOF samples were quickly washed with acetone three times and dried under a vacuum. The samples were then digested in a heated sonicator using 1 mL of a 3:1 solution of nitric acid and hydrogen peroxide. The resulting samples were diluted to 25 or 50 mL using Millipore water.

Table S2. ICP Results of Digested MOFs Pre- and Post-catalysis.

Sample Name	MOF Sample Mass (mg)	Volume (mL)	Zr weight %	Sn/In weight %	In/Zr_6 or Sn/Zr_6 Molar Ratio
PCN-222(Sn)_pre	1.69	50	15.6	6.7	1.97
PCN-222(Sn)_post	2.10	50	14.8	5.0	1.57
PCN-222(In)_pre	1.22	50	17.5	3.3	0.89
PCN-222(In)_post	1.98	50	15.7	2.4	0.73
CSLA-21(Sn)_pre	1.54	50	16.2	9.1	2.58
CSLA-21(Sn)_post	0.78	25	22.0	2.9	0.62
CSLA-21-NH_2(Sn)_pre	1.16	50	6.0	18.4	14.13
CSLA-21-NH_2(Sn)_post	1.19	50	7.3	15.1	9.54

Section S10. ROS Generation and Trapping Experiments

Singlet Oxygen ($^1O_2$) Trapping. A stock solution of 4.85 mM 9,10-dimethylanthracene (DMA) was prepared by dissolving 8.0 mg of DMA in 8 mL of MeOH through sonication. The stock solution was then diluted in MeOH to 0.08 mM. 1 mL of the diluted solution was added to 7 mL of MeOH to obtain an absorbance of about 0.8 in the 360 to 400 nm range.

To respective microwave vials containing 6 mL of the dilute DMA solution, MOFs were added. The vial was capped with a rubber septum and bubbled with O_2 for 1 minute. The vial was centrifuged, the septum was removed, and 3 mL of the solution was filtered into a quartz cuvette and analyzed using a UV-Vis spectrometer to provide t = 0 min. After analysis, the quartz tube was emptied back into the microwave vial. The vial was then capped, and oxygen was flushed while the vial was irradiated by a halogen lamp with a 493 nm cutoff filter. Aliquots were similarly collected at t = 15, 30, and 45 min for PCN-222(In), CSLA-21(Sn), and CSLA-21-NH_2(Sn) and at t = 2, 4, and 6 min for PCN-222(FB) and PCN-222(Sn).

Radical ($\bullet O_2^-$/$\bullet$OH) Trapping. The presence of free radicals was determined via the bleaching of *N,N*-dimethyl-4-nitrosoaniline (DMNA) following a procedure modified from Wang et al.[22] A 1.6 mM stock solution of DMNA was prepared in MeOH. From this stock solution, a 0.250 mM solution in MeCN was prepared.

To a microwave vial, 2 mL of 0.250 mM DMNA in MeCN were added along with 0.001 mmol of MOF catalyst. The suspension was sonicated in the dark, and then O_2 gas was bubbled into the vial for 20 min. This was immediately followed by irradiation using blue LEDs for 10 min. Upon completion, the vial was centrifuged, and 1 mL of the suspension was filtered through a 0.22 μm syringe filter into a UV cuvette. 2 mL of MeCN was added, and the absorbance was measured from 300-500 nm. A control was run similarly without the addition of MOF.

Peroxide (H_2O_2) Trapping. The presence of peroxides was determined via the formation of triiodide following a procedure modified from Wang et al.[22] The detection solution was prepared using potassium iodide (33 g/L), sodium hydroxide (1 g/L), ammonium molybdate tetrahydrate (0.1 g/L), and potassium hydrogen phthalate (10 g/L).

To a microwave vial, the MOF catalyst and 1 mL MeOH were added. The suspension was sonicated in the dark, bubbled with O_2 for 20 minutes, and irradiated with blue LED light for 20 minutes. 2 mL of trap solution was immediately added after irradiation with blue LED. The vial was then centrifuged, and 1 mL of the suspension was filtered into a separate vial where 4 mL of MeOH was then added. The absorbance of the filtered solution was then measured from 300-400 nm. A control was run similarly without the addition of MOF.

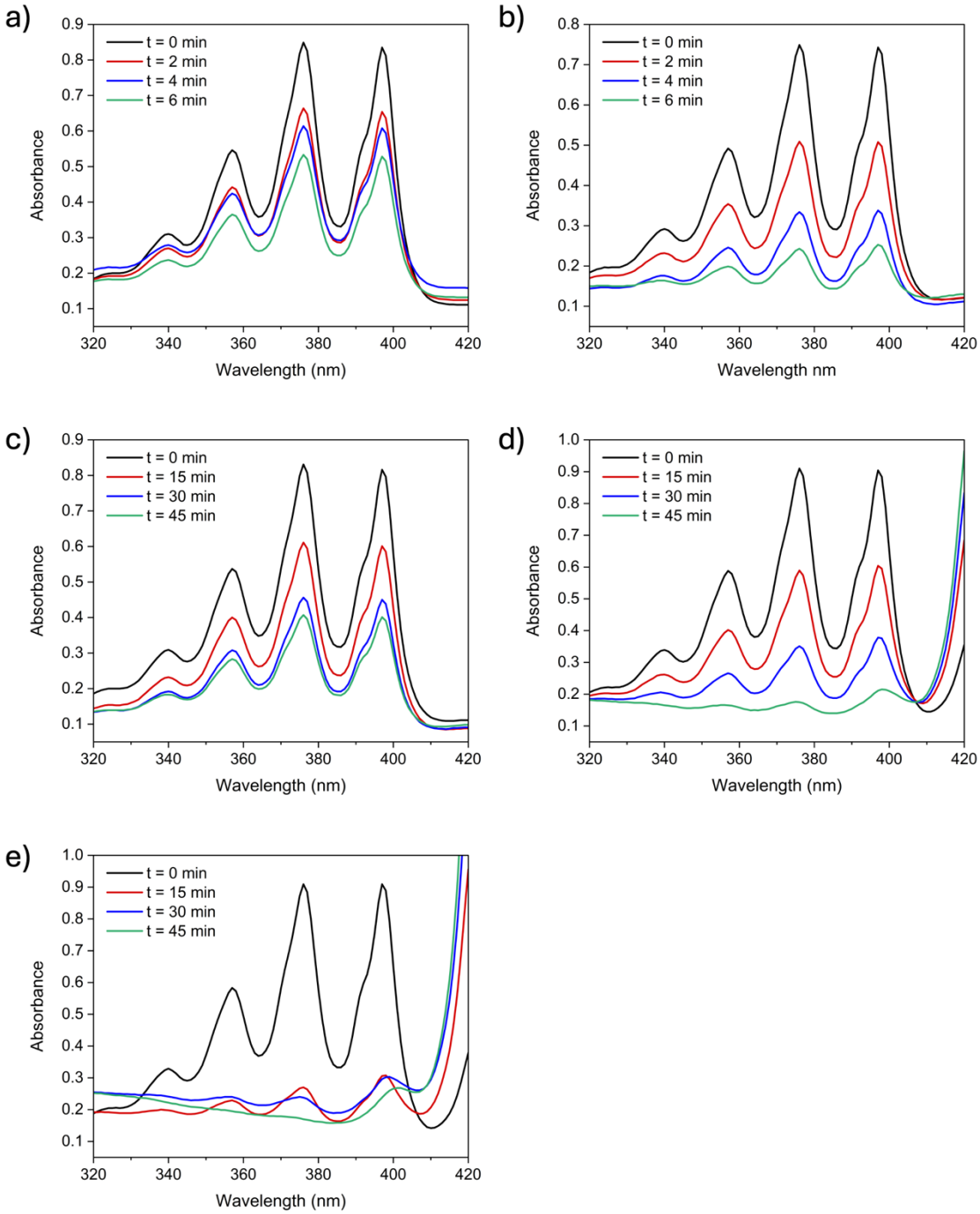

Figure S17. Singlet oxygen trapping experiments using (a) PCN-222(free base), (b) PCN-222(Sn), (c) PCN-222(In), (d) CSLA-21(Sn), and (e) CSLA-21-NH_2(Sn) indicating the oxidation of 9,10-dimethylanthracene (DMA) into DMA-O_2 over time.

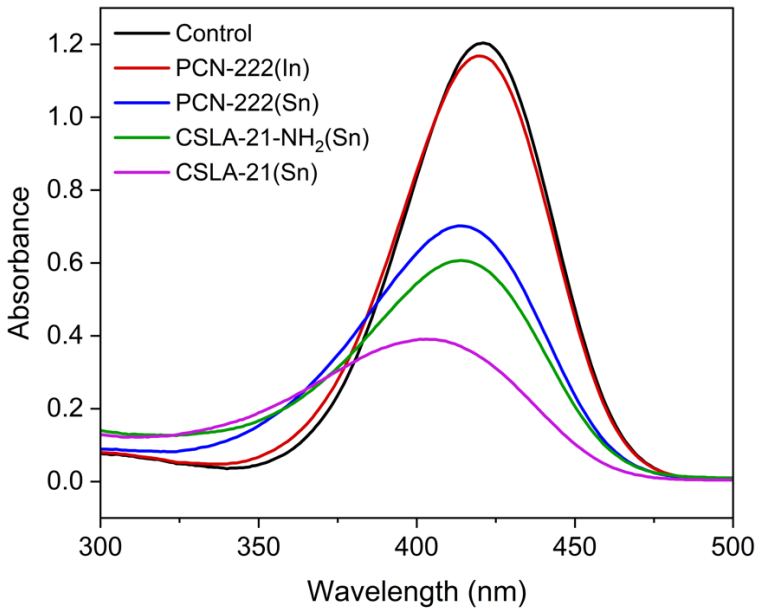

Figure S18. Radical trapping experiments indicating the bleaching of *N*,*N*-dimethyl-4-nitrosoaniline (DMNA).

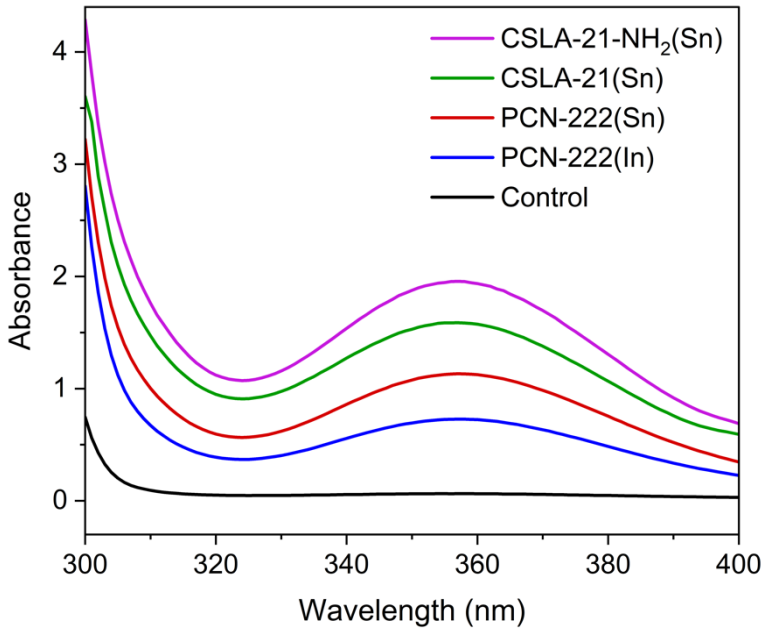

Figure S19. Peroxide trapping experiments indicating the formation of triiodide.

Section S11. X-ray photoelectron spectroscopy (XPS)

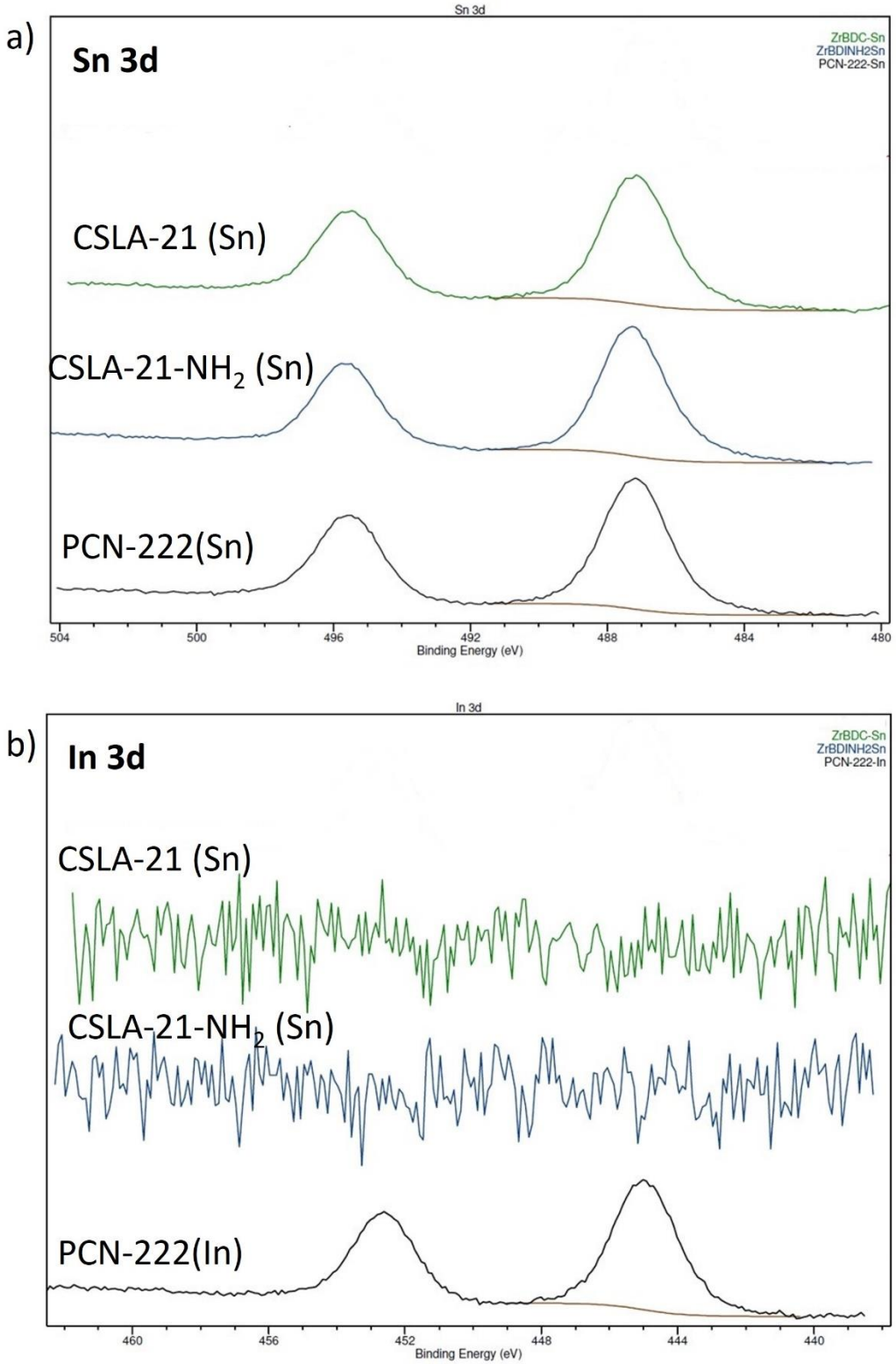

Figure S20. X-ray photoelectron spectroscopy (Sn 3d and In 3d) for all MOF samples.

Table S3. XPS Results

Sample Name	Oxidation State
PCN-222(Sn)	Sn^{4+}
PCN-222(In)	In^{3+}
CSLA-21(Sn)	Sn^{4+}
CSLA-21-NH_2(Sn)	Sn^{4+}

References

1. A.-M. Manke, K. Geisel, A. Fetzer and P. Kurz, *Phys. Chem. Chem. Phys.*, 2014, **16**, 12029-12042.
2. D. Feng, Z. Y. Gu, J. R. Li, H. L. Jiang, Z. Wei and H. C. Zhou, *Angew. Chem. Int. Ed.*, 2012, **51**, 10307-10310.
3. S. Leubner, H. Zhao, N. Van Velthoven, M. Henrion, H. Reinsch, D. E. De Vos, U. Kolb and N. Stock, *Angew. Chem. Int. Ed.*, 2019, **58**, 10995-11000.
4. Y. Hao, E. K. Papazyan, Y. Ba and Y. Liu, *ACS Catal.*, 2022, **12**, 363-371.
5. M. M. Wu, J. Su, D. Luo, B. C. Cai, Z. L. Zheng, D. S. Bin, Y. Y. Li and X. P. Zhou, *Small*, 2023, **19**, 2301050.
6. C.-H. Gong, Z.-B. Sun, M. Cao, X.-M. Luo, J. Wu, Q.-Y. Wang, S.-Q. Zang and T. C. W. Mak, *Chem. Commun.*, 2022, **58**, 9806-9809.
7. H. Zhao, C.-A. Tao, S. Zhao, X. Zou, F. Wang and J. Wang, *ACS Appl. Mater. Interfaces*, 2023, **15**, 3297-3306.
8. J. Zhou, X. Li, C. Chu and J. Cao, *Microporous Mesoporous Mater.*, 2024, **375**, 113163.
9. M. Cao, R. Pang, Q.-Y. Wang, Z. Han, Z.-Y. Wang, X.-Y. Dong, S.-F. Li, S.-Q. Zang and T. C. W. Mak, *J. Am. Chem. Soc.*, 2019, **141**, 14505-14509.
10. W. Wu, T. He, X. Zhang, L.-H. Xie, G.-R. Si, Y. Xie and J.-R. Li, *Inorg. Chem.*, 2024, **63**, 7412-7421.
11. M. S. Lee, S. J. Garibay, A. M. Ploskonka and J. B. Decoste, *MRS Commun.*, 2019, **9**, 464-473.
12. A. Atilgan, T. Islamoglu, A. J. Howarth, J. T. Hupp and O. K. Farha, *ACS Appl. Mater. Interfaces*, 2017, **9**, 24555-24560.
13. Z.-H. Long, D. Luo, K. Wu, Z.-Y. Chen, M.-M. Wu, X.-P. Zhou and D. Li, *ACS Appl. Mater. Interfaces*, 2021, **13**, 37102-37110.
14. W.-Q. Zhang, K. Cheng, H. Zhang, Q.-Y. Li, Z. Ma, Z. Wang, J. Sheng, Y. Li, X. Zhao and X.-J. Wang, *Inorg. Chem.*, 2018, **57**, 4230-4233.
15. A. J. Howarth, C. T. Buru, Y. Liu, A. M. Ploskonka, K. J. Hartlieb, M. McEntee, J. J. Mahle, J. H. Buchanan, E. M. Durke, S. S. Al-Juaid, J. F. Stoddart, J. B. Decoste, J. T. Hupp and O. K. Farha, *Chem. - Eur. J.*, 2017, **23**, 214-218.
16. S. Goswami, C. E. Miller, J. L. Logsdon, C. T. Buru, Y.-L. Wu, D. N. Bowman, T. Islamoglu, A. M. Asir, C. J. Cramer, M. E. Wasielewski, J. T. Hupp and O. K. Farha, *ACS Appl. Mater. Interfaces*, 2017, **9**, 19535-19540.
17. C. T. Buru, M. B. Majewski, A. J. Howarth, R. H. Lavroff, C.-W. Kung, A. W. Peters, S. Goswami and O. K. Farha, *ACS Appl. Mater. Interfaces*, 2018, **10**, 23802-23806.
18. D. T. Lee, J. D. Jamir, G. W. Peterson and G. N. Parsons, *Matter*, 2020, **2**, 404-415.
19. J. F. Zhou, J. J. Ling, G. Li, S. Zhang and D. Zhu, *Mater. Today Chem.*, 2022, **24**, 100774.
20. A. M. Kulisiewicz, S. J. Garibay, G. R. Pozza, M. A. Browe, O. Sparr, S. Singh, L. A. Kelly and J. B. Decoste, *ACS Appl. Mater. Interfaces*, 2023, **15**, 40727-40734.
21. Y. Liu, C. T. Buru, A. J. Howarth, J. J. Mahle, J. H. Buchanan, J. B. Decoste, J. T. Hupp and O. K. Farha, *J. Mater. Chem. A*, 2016, **4**, 13809-13813.
22. Y. Wang, K. Ma, J. Bai, T. Xu, W. Han, C. Wang, Z. Chen, K. O. Kirlikovali, P. Li, J. Xiao and O. K. Farha, *Angew. Chem. Int. Ed.*, 2022, **61**, e202115956.